Temperature dependence of the direct interband transitions of a Ge/SiGe multiple-quantum-well structure with Ge-rich barriers

P. H. Wu,[1] Y. S. Huang,[1,*] H. P. Hsu,[2] D. Chrastina,[3] G. Isella,[3] H. von Känel,[3] and K. K. Tiong[4]
[1]*Department of Electronic Engineering, National Taiwan University of Science and Technology, Taipei 106, Taiwan*
[2]*Department of Electronic Engineering, Ming Chi University of Technology, Taishan, Taipei 243, Taiwan*
[3]*L-NESS, Dipartimento di Fisica del Politecnico di Milano, Polo di Como, via Anzani 42, I-22100 Como, Italy*
[4]*Department of Electrical Engineering, National Taiwan Ocean University, Keelung 202, Taiwan*
(Received 30 October 2011; revised manuscript received 21 December 2011; published 5 January 2012)

Temperature-dependent piezoreflectance (PzR) measurements were used to study the direct-gap–related optical transitions in a strain-compensated Ge/SiGe multiple-quantum-well (MQW) structure with Ge-rich SiGe barriers in the temperature range between 20 and 375 K. The PzR spectra revealed a wide range of possible optical transitions in the MQW structure. Detailed line-shape fits to the PzR spectra and comparison to a theoretical calculation based on the envelope-function approximation led to the identification of various interband transitions. In addition, the parameters that describe the temperature dependence of the excitonic transition energies [E(T)] and broadening parameters [Γ(T)] were evaluated and compared to those of the polar systems. In agreement with polar materials, [E(T)] values of the MQW structure were found to be similar to the constituent bulk well material. On the other hand, no significant dimensionality dependence of [Γ(T)] was observed, in contrast to polar systems.

DOI: 10.1103/PhysRevB.85.035303 PACS number(s): 78.40.−q, 78.67.De

I. INTRODUCTION

Recent progress in Si photonics[1–3] suggests that Si-based materials could provide strong support for the technological integration of optical functions in complementary metal-oxide-semiconductor (CMOS) microelectronics.[4] In this perspective, SiGe alloys are of particular interest because they can be epitaxially grown on Si substrates and are compatible with a large number of standard Si processes and CMOS technology.[5] Bulk mobilities of SiGe alloys with high Ge content are higher than those of Si for both electron and holes.[6] Moreover, SiGe technology allows the integration on Si substrates of high-speed electronic devices, such as high-electron-mobility transistors,[7] modulation-doped field effect transistors,[8] and heterojunction bipolar transistors.[9]

In Ge, the direct gap at the Γ point is only 140 meV above the indirect fundamental gap at room temperature,[10] and the direct gap energy is within the range of wavelengths used in telecommunications. Ge/SiGe multiple-quantum-well (MQW) structures with Ge-rich barriers have attracted more attention because their optical properties are expected to exhibit close analogies to those of III-V direct-gap semiconductors.[11–17] Yaguchi *et al.*[18] showed quantum confinement in Ge/SiGe MQW grown on Ge substrates by photoreflectance spectroscopy at 120 K in 1994. Recently, a strong quantum Stark effect associated with the direct-gap interband transition has been observed in strained Ge/SiGe MQW on relaxed Ge-rich SiGe buffers by photocurrent and transmission spectroscopy, and electro-absorption modulators based on this effect have also been demonstrated.[19,20] Furthermore, Gatti *et al.*[21] reported the observation of room-temperature direct-band-gap photoluminescence in compressively strained Ge MQW with Ge-rich SiGe barriers. Their results show that Ge/SiGe MQWs can be promising candidates for efficient light-emitting devices monolithically integrated on Si.

In this paper, we report a detailed temperature-dependent piezoreflectance (PzR) characterization on a Ge/SiGe MQW structure with Ge-rich barriers grown by low-energy plasma-enhanced chemical vapor deposition (LEPECVD)[22] in the temperature range between 20 and 375 K. PzR has been proven to be useful in the characterization of semiconductor microstructures.[23,24] The derivative nature of PzR spectra suppresses uninteresting background effects and greatly enhances the precision of the determination of interband transition energies. The sharper line shapes as compared to the conventional optical techniques enabled us to achieve a greater resolution and hence to detect weaker features. The PzR spectra were fitted with a form of the Aspnes equation of the first-derivative Lorentzian line-shape form.[25] From a detailed line-shape fit, we have been able to accurately measure the temperature dependence of the energies and broadening parameters [Γ(T)] of the interband excitonic transitions in the QWs. We have analyzed the temperature variation of the transition energies using the Varshni equation[26] and an expression containing the Bose-Einstein occupation factor for phonons.[27] The temperature dependence of the broadening function has also been studied in terms of a Bose-Einstein equation that contains the electron (exciton)-phonon-coupling constant.[23] The parameters that describe the excitonic transition energies and broadening function are evaluated and discussed.

II. EXPERIMENTAL DETAILS

The samples used in this study were grown by LEPECVD on 100 mm Si(001) substrates. The sample consists of 50 compressively strained 15-nm-wide Ge QWs. They are separated by 21-nm-thick $Si_{0.15}Ge_{0.85}$ barriers. The compressive (tensile) strain in the QW (barrier) layers is set by a fully relaxed virtual substrate (VS). The VS consists of a buffer layer graded from Si to $Si_{0.1}Ge_{0.9}$ over a thickness of 13 μm and capped with a 2 μm $Si_{0.1}Ge_{0.9}$ layer. The schematic MQW structure is shown in Fig. 1. The nominal well and barrier thicknesses and

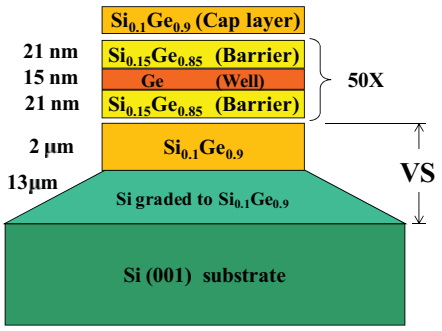

FIG. 1. (Color online) Schematic diagram of the $Ge/Si_{0.15}Ge_{0.85}$ MQW structure deposited on virtual substrate.

the barrier composition were determined by high-resolution x-ray diffraction.

For the PzR measurements, a thin sample of $\sim$100 μm was prepared by removing part of the Si substrate with successively finer grades of silicon carbide grinding papers. The thin sample was then was glued on a 0.15-cm-thick lead zirconate titanate piezoelectric transducer driven by a 100 V_{rms} sinusoidal source at 200 Hz. The alternating expansion and contraction of the transducer subjected the sample to an alternating strain in the plane perpendicular to the growth direction with a typical root mean square $\Delta l/l$ value of $\sim 10^{-5}$. The radiation from a 150 W tungsten-halogen lamp filtered by a 0.25 m monochromator provided the monochromatic light. The reflected light was detected by an InGaAs photodiode. The direct current (dc) output of this photodiode was maintained constant using a servomechanism of a variable neutral density filter. A dual-phase lock-in amplifier was used to measure the detected signals. Multiple scans over a given photon energy range were programmed until a desired signal-to-noise level was attained with computer-controlled data acquisition procedure. A closed-cycle cryogenic refrigerator equipped with a digital temperature controller was used for the low-temperature measurements. For the high-temperature experiments, the sample was mounted on one side of a copper finger of an electrical heater, which enabled us to control and stabilize the sample temperature. The temperature-dependent measurements were made between 20 and 375 K with temperature stability of 0.5 K or better.

III. RESULTS AND DISCUSSION

In Figs. 2(a) and 2(b), the dashed curves represent the experimental PzR spectra of a 50 period strain-compensated Ge/SiGe MQW structure at 300 and 20 K, respectively. As can be seen in Fig. 2, the optical transitions related to the MQW are observed, as well as transitions corresponding to the split band-gap energies of the $Si_{0.15}Ge_{0.85}$ barriers. Since the band-gap energies of the barrier layers are measured directly, the barrier height can be determined accurately without using the literature values. The direct determination of barrier heights from experiment is desirable since the band-gap energy of the barrier layers or deformation potentials may cause some errors in the calculation of the quantum levels. In order to determine interband transition energies from the PzR spectra, we fitted the experimental data with the first-derivative

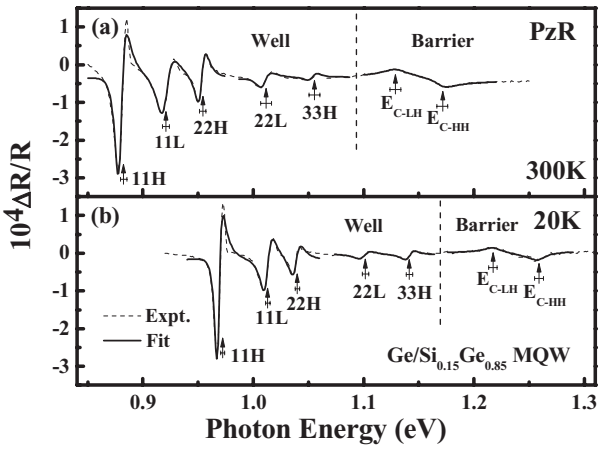

FIG. 2. The experimental PzR spectra (dashed curves) at (a) 300 and (b) 20 K of the $Ge/Si_{0.15}Ge_{0.85}$ MQW structure. The solid curves are the least-squares fits to Eq. (1). The arrows indicate all the transition energies resulting from the fits. Error bars are indicated.

Lorentzian line-shape (FDLL) function. The solid curves are the least-squares fits to FDLL function of the form[25,28]

$$\frac{\Delta R}{R} = \mathrm{Re}\sum_{j=1} A_j e^{i\Phi_j}(E - E_j + i\Gamma_j)^{-n}, \qquad (1)$$

where A_j and Φ_j are the amplitude and phase of the line shape, E_j and Γ_j are the energy and broadening parameters of the transitions, and the value of n depends on the origin of the transitions, with n = 0.5 being appropriate for M_0-type three-dimensional critical point interband transitions and n = 2 appropriate for the bounded transitions.[25,28] Our experimental signatures for the light-hole and heavy-hole band-gap energies of the barrier layers, denoted as $E_{C\text{-}LH}$ and $E_{C\text{-}HH}$, are more consistent with n = 0.5, while the features originating from MQW interband excitonic transitions have better fit with n = 2. The arrows with error bars in Fig. 2 indicate all the energy values of the transitions resulting from the fits. In this work, the compressive strain in MQW breaks the degeneracy of heavy-hole and light-hole states in the valence band. The interband excitonic transitions observed in PzR spectra in the MQW regime are labeled as mnH(L) by arrows. Here, m is the quantum-confined electron m^{th} subband in the conduction band at the Γ point, and nH(L) represents the heavy- and light-hole n^{th} subband. The transition energies obtained from the PzR spectra of the Ge/SiGe MQW at 300 and 20 K are listed in Table I. As can be seen in Fig. 2, the amplitude of the 11H transition is larger than that of the 11L transition, where the fitted value of A_{11H}/A_{11L} = 2.8 and 2.9 at 300 and 20 K, respectively. The amplitude ratio between 11H and 11L features can be understood as follows. For the present experimental configuration, the ratio of the bulk transition matrix elements for heavy-hole and light-hole transitions is 3:1. It is known that the ratio of the oscillator strengths of heavy-hole and light-hole excitonic transitions in QWs depends on the bulk transition matrix elements and the overlap of the envelope functions of the confined electron states and the confined hole states. The overlap of the envelope functions between the first confined electron state and the first confined

TABLE I. Transition energies obtained from PzR spectra of a $Ge/Si_{0.15}Ge_{0.85}$ strained-compensated MQW structure measured at 300 and 20 K. The nominal well and barrier thicknesses were 15 and 21 nm, respectively. Theoretical values were calculated for the conduction-band-offset ratio $Q_c = 0.68$. The strain-compensated factor $\gamma = 0.1$ was included in this calculation.

	Experimental (eV)		Theory (eV)
Transition	300 K	20 K	300 K
11H	0.880 ± 0.003	0.968 ± 0.002	0.881
11L	0.920 ± 0.003	1.013 ± 0.002	0.920
22H	0.953 ± 0.003	1.039 ± 0.002	0.959
22L	1.009 ± 0.005	1.101 ± 0.003	1.027
33H	1.054 ± 0.005	1.141 ± 0.003	1.070
Barrier ($E_{C\text{-}LH}$)	1.129 ± 0.005	1.217 ± 0.005	
Barrier ($E_{C\text{-}HH}$)	1.171 ± 0.005	1.259 ± 0.005	

heavy-hole/light-hole state in MQW is found to be similar. The oscillator strength of the intersubband transition is also known to be proportional to the amplitude A times the line-width parameter Γ. It is noted that the line width for the 11L transition is larger than that of the 11H transition. Typically, the light-hole transitions are more sensitive to biaxial strain variations, which may have origins from either intrinsic strain fluctuations in the sample, or they may be induced by the piezomodulation mechanism. It is known that the modulation mechanism may also affect the line width observed in the piezomodulated spectrum. Another possible reason for the larger line width of light-hole transitions is the larger overlap of the light-hole wave function with the SiGe barrier, i.e., alloy broadening.

Figure 3 depicts the lineup of various relevant bands at the Γ point in a strain-compensated structure of a Ge well between $Si_{0.15}Ge_{0.85}$ barriers on a $Si_{0.10}Ge_{0.90}$ strain-relaxed virtual substrate. The compressive strain in the Ge wells causes the HH band to shift up, the LH band to shift down, and an overall increase in the band gap. On the other hand, the tensile strain in the $Si_{0.15}Ge_{0.85}$ barrier layers shifts the HH and LH bands opposite to that of the Ge well and decreases the overall band gap. By strain compensating, stability is maintained in the structure, and hence uniform QWs are achieved. The corresponding band offsets of the conduction, heavy-hole

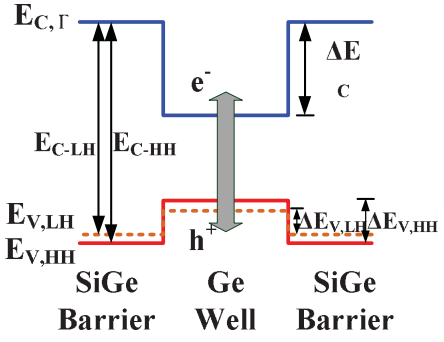

FIG. 3. (Color online) The lineup of various relevant bands at the Γ point in a strain-compensated structure of a Ge well between $Si_{0.15}Ge_{0.85}$ barriers on a $Si_{0.10}Ge_{0.90}$ strain-relaxed virtual substrate.

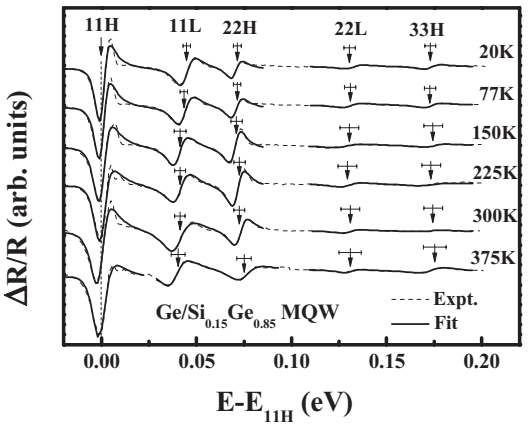

FIG. 4. The dashed curves are the experimental PzR spectra at various temperatures in the region of interband transitions of a $Ge/Si_{0.15}Ge_{0.85}$ MQW structure. The solid curves are least-squares fits to Eq. (1), yielding the energies indicated by arrows. For clarity, the zero of energy is the energy of the 11 H transition at each temperature. Error bars are indicated.

valence, and light-hole valence bands are denoted as ΔE_C, $\Delta E_{V,HH,}$ and $\Delta E_{V,LH,}$ respectively, as indicated in Fig. 3. The band alignment of both heavy- and light-hole valence bands at the Γ point is of type I.

To assign the observed interband transitions, a calculation was performed based on the envelope function approximation.[29] Following the previously reported value for the conduction-band-offset Q_c at the Γ point,[18] we have assumed that the Q_c is 0.68 ± 0.08 of the band-gap difference between the barriers and wells. In order to analyze the experimental results, an adjustable strain compensation factor γ has been introduced and defined as $\gamma = (1 - \frac{\varepsilon'}{\varepsilon})$, where ε' is the effective strain, and ε is the coherent strain. The strain compensation factor lies in between zero and unity, i.e., $0 \leqslant \gamma \leqslant 1$, where $\gamma = 0$ corresponds to fully strained and $\gamma = 1$ is fully relaxed. We have used a number of relevant parameters for Si and Ge listed in Ref. 30. The lattice constant, hydrostatic (a) and shear (b) deformation potentials, the effective mass of electron, heavy-hole and light-hole, and the elastic stiffness constants C_{11} and C_{12} of the binary materials were obtained by linear interpolation of values of the end-point semiconductors Si and Ge. The calculated transition energies are also listed in Table I.

The PzR spectra of the MQW structure in the spectral range of five interband transitions at 20, 77, 150, 225, 300, and 375 K, respectively, are shown in Fig. 4. To facilitate comparison of spectra at different temperatures, we have taken the zero of energy of each scan to lie at the 11H transition energy. The identifications denoted by 11H, 11L, 22H, 22L, and 33 H are indicated by arrows at the top of the figure. Error bars are included. It is noted that there is no obvious change in the relative position of each transition as the temperature is varied.

The temperature dependence of $E_{mnH(L)}(T)$ is plotted in Fig. 5. The solid lines are the least-squares fits to the Varshni semi-empirical relationship:[26]

$$E(T) = E(0) - \alpha T^2/(\beta + T), \quad (2)$$

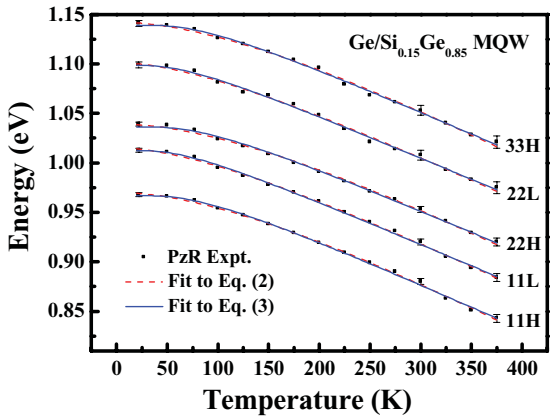

FIG. 5. (Color online) Temperature dependence of various interband excitonic transition energies for a $Ge/Si_{0.15}Ge_{0.85}$ MQW structure. The dashed lines and solid lines are the least-squares fits to Eqs. (2) and (3), respectively. Representative error bars are indicated.

where E(0) are the energies for the mnH(L) transition at 0 K, and α and β are the Varshni coefficients. The constant α is related to the electron (exciton)-average phonon interaction, and β is closely related to the Debye temperature.[26] The obtained values of E(0), α, and β are listed in Table II. For comparison, we have also listed in Table II the values of E(0), α, and β for Ge,[23] Ge-rich $(Si)_m/(Ge)_n$,[31] and Ge/SiGe MQW.[23]

We have also fitted the experimental data to a Bose-Einstein expression:[27]

$$E(T) = E(0) - \frac{2a_B}{[\exp(\Theta_B/T) - 1]}, \quad (3)$$

where E(0) is the transition energy of mnH(L) at 0 K, a_B represents the strength of the electron-phonon interaction, and Θ_B corresponds to the average phonon temperature. The obtained values of E(0), a_B, and Θ_B are listed in Table II, along with the corresponding values for the direct gaps of Ge[23] and Ge/SiGe MQW.[23] The values of a_B and Θ_B in our sample are fairly similar to those of Ge bulk. For heavy holes and light holes, there are slight differences in the fitted values of a_B and Θ_B. We interpret this as being the result of lighter effective mass of light holes. The light holes are therefore more sensitive to confinement changes, i.e., the reduction of the potential height with temperature. Since the differences are within the probable errors of measurement, a detailed comparison of these parameters is difficult to perform. Our observation that the temperature dependence of interband transition energies in reduced dimensional systems is essentially the same as the constituent bulk material is consistent with most of the previous reports,[23,32,33] except for Ref. 31. It should be noted that the line-shape function used in Ref. 31, a third-derivative Lorentzian line-shape function, did not fit the experimental data well, which may have introduced errors in determining the transition energies. However, the reason why the temperature variations of band gaps are independent of dimensionality has not yet been explained on a theoretical basis.

From Eq. (3), it is straightforward to show that high-temperature limit of the slope of the E(T) versus T curve approaches a value of $-2a_B/\Theta_B$. The calculated value of $-2a_B/\Theta_B$ for the 11H and 11L transition equals -0.47 meV/K and -0.46 meV/K, respectively, which agree well with the values of $dE_{11H}/dT = -0.45$ meV/K and $dE_{11L}/dT = -0.44$ meV/K as obtained from the linear extrapolation

TABLE II. Values of parameters E(0), α, β, a_B, and Θ_B, which describe the temperature dependence of the energies of the various transitions of a strain-compensated $Ge/Si_{0.15}Ge_{0.85}$ MQW structure. The parameters for Ge, Ge-rich $(Si)_m/(Ge)_n$, and Ge/SiGe MQW are listed for comparison.

Transitions	E(0) (eV)	α ($\times 10^{-4}$ eV/K)	β (K)	a_B (meV)	Θ_B (K)
11H	0.9680 ± 0.003	7.4 ± 0.8	430 ± 100	59 ± 10	250 ± 30
11L	1.011 ± 0.003	7.2 ± 0.8	400 ± 100	56 ± 10	245 ± 30
22H	1.037 ± 0.003	6.9 ± 0.8	430 ± 100	55 ± 10	250 ± 30
22L	1.097 ± 0.003	7.0 ± 0.9	410 ± 100	56 ± 10	240 ± 30
33H	1.139 ± 0.003	7.2 ± 0.9	430 ± 100	57 ± 10	250 ± 30
E_0^{BB}(Ge)	0.8853 ± 0.002[a]	6.5 ± 0.7[a]	410 ± 100[a]	70 ± 10[a]	302 ± 35[a]
	0.892[b]	7.25[b]	433[b]		
	0.8893[c]	6.84[c]	398[c]		
11H[b,d]	1.33	9.56	598		
11L[b,d]	1.23	4.35	147		
11H[a,e]	0.957 ± 0.003	7.2 ± 1.5	420 ± 150	65 ± 10	290 ± 46
11L[a,e]	0.984 ± 0.003	6.8 ± 1.5	370 ± 150	60 ± 10	255 ± 46
11H[a,f]	1.062 ± 0.003	8.4 ± 1.0	566 ± 120	80 ± 10	313 ± 35
11L[a,f]	1.091 ± 0.003	8.2 ± 1.0	555 ± 120	82 ± 10	313 ± 35

[a]Reference 23 (piezoreflectance).
[b]Reference 31 (photoreflectance).
[c]Reference 26 (transmittance).
[d]Ge-rich $(Si)_m/(Ge)_n$ superlattice.
[e]$(Si_4Ge_6)_5Ge_{78}$ MQW.
[f]$(Si_3Ge_7)_5Ge_{29}$ MQW.

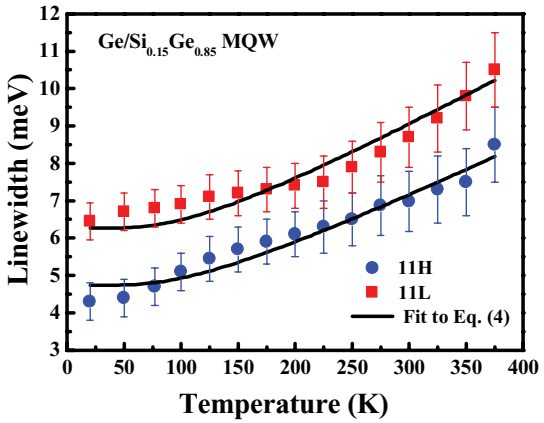

FIG. 6. (Color online) Temperature-dependent broadening parameters Γ(T) of 11H (closed circles) and 11L (closed squares) features for a $Ge/Si_{0.15}Ge_{0.85}$ MQW structure. The solid lines are the least-squares fits to Eq. (4) with the dominant longitudinal acoustic phonons energy $E_{LA} = 28$ meV. Error bars are indicated.

of the high-temperature (225−375 K) PzR experimental data.

The temperature dependence of broadening parameters Γ(T) is a consequence of the electron (exciton)-phonon scattering process. The scattering processes related to the fundamental transition for Ge and Ge/SiGe MQW structures were reported to be well described by the following expression,[23] where the electron (exciton) scattering via the longitudinal acoustic phonons is the dominant process.[34,35]

$$\Gamma(T) = \Gamma(0) + \Gamma_p/[\exp(E_{LA}/kT) - 1], \quad (4)$$

where Γ(0) represents the broadening invoked from temperature-independent mechanisms, such as compositional fluctuations, alloy scattering, electron-electron interaction, impurity, and dislocation, Γ_p is the electron (exciton)-phonon coupling constant, and E_{LA} is the energy of longitudinal acoustic phonons.

The variations of the line width as a function of temperature Γ(T) of 11H (closed circles) and 11L (closed square) as obtained from the line-shape fit are plotted in Fig. 6. Representative errors bars are indicated. The full curves in Fig. 6 are least-squares fits to Eq. (4) to evaluate Γ(0) and Γ_p for both the 11H and 11L features. The fitted values of Γ(0) and Γ_p are listed in Table III. For comparison, the values of Γ_p for Ge,[23] Ge/SiGe MQW,[23] GaAs,[36] and GaAs/AlGaAs single-quantum-well (SQW)[36] from literature are also included in Table III. The fitted value of Γ(0) for 11L (6.5 ± 0.6 meV) is found to be much larger than that of 11H (4.7 ± 0.6 meV). The obtained values of Γ_p for 11H and 11L are similar and equal to 4.7 ± 1.0 meV. These numbers are similar to that of the direct band-edge transition feature for Ge.[23] In contrast to polar system materials such as GaAs,[36] our results revealed no significant dimensionality dependence of Γ_p. It is known that the electron (exciton) coupling constant for nonpolar material Ge (∼4 meV)[23] is much smaller than the corresponding value for the direct gap of polar material GaAs (∼20 meV).[36] In polar semiconductors, the electron (exciton)–optical phonon coupling is due to the long-range

TABLE III. Values of Γ(0) and Γ_p that describe the temperature dependence of the broadening function Γ(T) for 11H and 11L excitonic transitions of a strain- compensated $Ge/Si_{0.15}Ge_{0.85}$ MQW structure obtained from Eq. (4) with $E_{LA} = 28$ meV. The values of Γ(0) and Γ_p for Ge, Ge/SiGe MQW, GaAs, and GaAs/AlGaAs SQW are listed for comparison.

Transition	Γ(0) (meV)	Γ_p (meV)
11H	4.7 ± 0.6	4.7 ± 1.0
11L	6.5 ± 0.6	4.7 ± 1.0
E_0^{BB}(Ge)	1.06 ± 0.15[a]	4.2 ± 0.8[a]
E_0^{ex}(Ge)	3.30 ± 0.35[a]	4.0 ± 1.2[a]
E_0(GaAs)	2.2 ± 0.2[b]	20 ± 1.0[b]
11H[a,c]	4.9 ± 0.5	3.5 ± 0.8
11L[a,c]	4.9 ± 0.5	3.2 ± 0.9
11H[a,d]	10.2 ± 0.6	5.4 ± 0.9
11L[a,d]	10.4 ± 0.6	4.4 ± 1.2
11H[b,e]		1.7 ± 0.9

[a]Reference 23 (piezoreflectance).
[b]Reference 36 (photoreflectance)
[c]$(Si_4Ge_6)_5Ge_{78}$ MQW.
[d]$(Si_3Ge_7)_5Ge_{29}$ MQW.
[e]GaAs/AlGaAs SQW, Well width 6 nm.

Fröhlich interaction,[36,37] which is stronger than the short-range deformation potential coupling. In reduced dimensional polar systems, the confinement of the optical phonons causes a decrease in the phase space for the long-range Fröhlich interaction, which leads to a decrease in Γ_p.[36] On the other hand, our experimental results agree well with the previous report by Yin *et al.*[23] that the short-range deformation potential interaction in nonpolar materials should have a much weaker dependence on dimensionality.

IV. SUMMARY

In summary, temperature-dependent PzR measurements were used to characterize a strain-compensated Ge/SiGe multiple-quantum-well structure with Ge-rich SiGe barriers in the temperature range between 20 and 375 K. Using PzR and theoretical envelope function approximation calculations, the ground state and higher-order interband excitonic transitions were observed and identified. In addition, the parameters that describe the temperature dependence of the excitonic transition energies and broadening parameters were evaluated and compared to those of the polar systems. In agreement with polar materials, E(T) values of the MQW structure were found to be similar to that of the constituent bulk well material. On the other hand, in contrast to polar systems, no significant dimensionality dependence of Γ(T) was observed.

ACKNOWLEDGMENTS

The authors acknowledge the support of the National Science Council of Taiwan under Project Nos. NSC 100-2112-M-011-001-MY3, NSC 100-2221-E-131-005-MY2, and NSC 100-2811-M-011-001.

*ysh@mail.ntust.edu.tw

[1]M. Haurylau, S. P. Anderson, K. L. Marshall, and P. M. Fauchet, IEEE J. Sel. Top. Quant. **12**, 1527 (2006).
[2]V. Švrček, T. Sasaki, Y. Shimizu, and N. Koshizaki, J. Appl. Phys. **103**, 023101 (2008).
[3]H. Rong, A. Liu, R. Jones, O. Cohen, D. Hak, R. Nicolaescu, A. Fang, and M. Paniccia, Nature **433**, 292 (2005).
[4]M. Bonfanti, E. Grilli, M. Guzzi, D. Chrastina, G. Isella, H. Von Känel, and H. Sigg, Physica E **41**, 972 (2009).
[5]F. Schäffler, Semicond. Sci. Technol. **12**, 1515 (1997).
[6]K. Ismail, M. Arafa, K. L. Saenger, J. O. Chu, and B. S. Meyerson, Appl. Phys. Lett. **66**, 1077 (1995).
[7]E. M. Chumbes, A. T. Schremer, J. A. Smart, Y. Wang, N. C. MacDonald, D. Hogue, J. J. Komiak, S. J. Lichwalla, R. E. Leoni, III, and J. R. Shealy, IEEE Tran. Electron. Dev. **48**, 420 (2001).
[8]H. Daembkes, H. J. Herzog, H. Jorke, H. Kibbel, and E. Kaspar, IEEE Tran. Electron. Dev. **33**, 633 (1986).
[9]P. Narozny, H. Dambkes, H. Kibbel, and E. Kasper, IEEE Tran. Electron. Dev. **36**, 2363 (1989).
[10]*Numerical Data and Functional Relationships in Science and Technology*, edited by O. Madelung, Landolt-Börnstein, New Series, Group III, Vol. 17, Pt. A (Springer-Verlag, Berlin, 1982).
[11]Y. H. Kuo, Y. K. Lee, Y. Ge, S. Ren, J. E. Roth, T. I. Kamins, D. A. B. Miller, and J. S. Harris, Nature (London) **437**, 1334 (2005).
[12]H. Kosaka, H. Shigyou, Y. Mitsumori, Y. Rikitake, H. Imamura, T. Kutsuwa, K. Arai, and K. Edamatsu, Phys. Rev. Lett. **100**, 096602 (2008).
[13]S. Tsujino, H. Sigg, G. Mussler, D. Chrastina, and H. von Känel, Appl. Phys. Lett. **89**, 262119 (2006).
[14]Y. Chen, C. Li, H. Lai, and S. Chen, Nanotechnology **21**, 115207 (2010).
[15]P. Chaisakul, D. Marrie-Morini, G. Isella, D. Chrastina, X. Le. Roux, S. Edmond, J. R. Coudevylle, E. Cassan, and L. Vivien, Optics Lett. **36**, 1794 (2011).
[16]Y. Rong, Y. Ge, Y. Huo, M. Fiorentino, M. R. T. Tan, T. I. Kamins, T. J. Oshalski, G. Huyet, and J. S. Harris Jr., IEEE J. Sel. Top. Quant. Electron. **16**, 85 (2010).
[17]Y. Chen, C. Li, Z. Zhou, H. Lai, S. Chen, W. Ding, B. Cheng, and Y. Yu, Appl. Phys. Lett. **94**, 141902 (2009).
[18]H. Yaguchi, K. Tai, K. Takemasa, K. Onabe, R. Ito, and Y. Shiraki, Phys. Rev. B **49**, 7394 (1994).
[19]D. J. Paul, Phys. Rev. B **77**, 155323 (2008).
[20]M. Bonfanti, E. Grilli, M. Guzzi, M. Virgilio, G. Grosso, D. Chrastina, G. Isella, H. von Känel, and A. Neels, Phys. Rev. B **78**, 041407 (2008).
[21]E. Gatti, E. Grilli, M. Guzzi, D. Chrastina, G. Isella, and H. von Känel, Appl. Phys. Lett. **98**, 031106 (2011).
[22]H. von Känel, M. Kummer, G. Isella, E. Müller, and T. Huckbarth, Appl. Phys. Lett. **80**, 2922 (2002).
[23]Y. Yin, D. Yan, F. H. Pollak, M. S. Hybertsen, J. M. Vandenberg, and J. C. Bean, Phys. Rev. B **52**, 8951 (1995).
[24]H. Mathieu, J. Allegre, and B. Gil, Phys. Rev. B **43**, 2218 (1991).
[25]F. H. Pollak and H. Shen, Mater. Sci. Eng. R Rep. **10**, xv (1993).
[26]Y. P. Varshni, Physica (Utrecht) **34**, 149 (1967).
[27]P. Lautenschlager, M. Garriga, S. Logothetidis, and M. Cardona, Phys. Rev. B **35**, 9174 (1987).
[28]D. E. Aspnes, in *Handbook of Semiconductors*, edited by M. Balkanski (North-Holland, Amsterdam, 1980), Vol. 2, p. 109.
[29]G. Bastard and J. A. Brum, IEEE J. Quant. Electron. **22**, 1625 (1986).
[30]S. Adachi, *Properties of Group-IV, III-V and II-VI Semiconductors* (John Wiley & Sons, New York, 2005), p. 178.
[31]P. A. Dafesh and K. L. Wang, Phys. Rev. B **45**, 1712 (1992).
[32]A. Kangarlu, H. R. Chandrasekhar, M. Chandrasekhar, Y. M. Kapoor, F. A. Chambers, B. A. Vojak, and J. M. Meese, Phys. Rev. B **37**, 1035 (1988).
[33]Y. S. Huang, H. Qiang, F. H. Pollak, G. D. Pettit, P. D. Kirchner, J. M. Woodall, H. Stragier, and L. B. Sorensen, J. Appl. Phys. **70**, 7537 (1991).
[34]G. G. Macfarlane, T. P. McLean, J. E. Quarrington, and V. Roberts, J. Phys. Chem. Solids **8**, 388 (1959).
[35]R. K. Schaevitz, D. S. Ly-Gagnon, J. E. Roth, E. H. Edvards, and D. A. B. Miller, AIP Adv. **1**, 032164 (2011).
[36]H. Qiang, F. H. Pollak, C. M. Sotomayer Torres, W. Leitch, A. H. Kean, M. A. Stroscio, G. J. Iafrate, and K. W. Kim, Appl. Phys. Lett. **61**, 1411 (1992).
[37]F. H. Pollak, in *Phonons in Semiconductor Nanostructures*, edited by J. P. LeBurton, J. Pasqual, and C. M. Sotomayer Torres (Kluwer, Dordrecht, Netherlands, 1993), p. 341.